

Resolution of rupture directivity in weak events: 1D versus 2D source parameterizations for the 2011, Mw 4.6 and 5.2 Lorca earthquakes, Spain

J. A. López-Comino^{1,2}, D. Stich^{2,3}, J. Morales^{2,3}, and A. M. G. Ferreira⁴

¹GFZ German Research Centre for Geosciences, Telegrafenberg, D-14473 Potsdam, Germany.

²Instituto Andaluz de Geofísica, Universidad de Granada, 18071 Granada, Spain

³Departamento de Física Teórica y del Cosmos, Universidad de Granada, 18071 Granada, Spain

⁴Department of Earth Sciences, Faculty of Maths & Physical Sciences, University College London, WC1E6BT, UK

Contents of this file

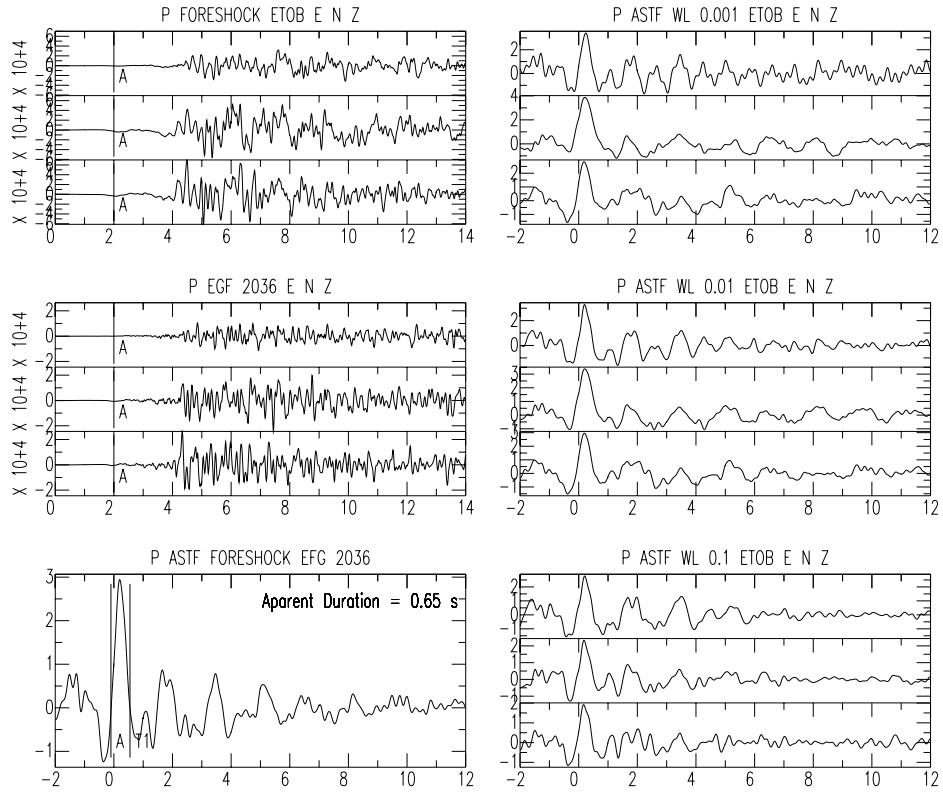
Figures S1 to S5

Tables S1 to S2

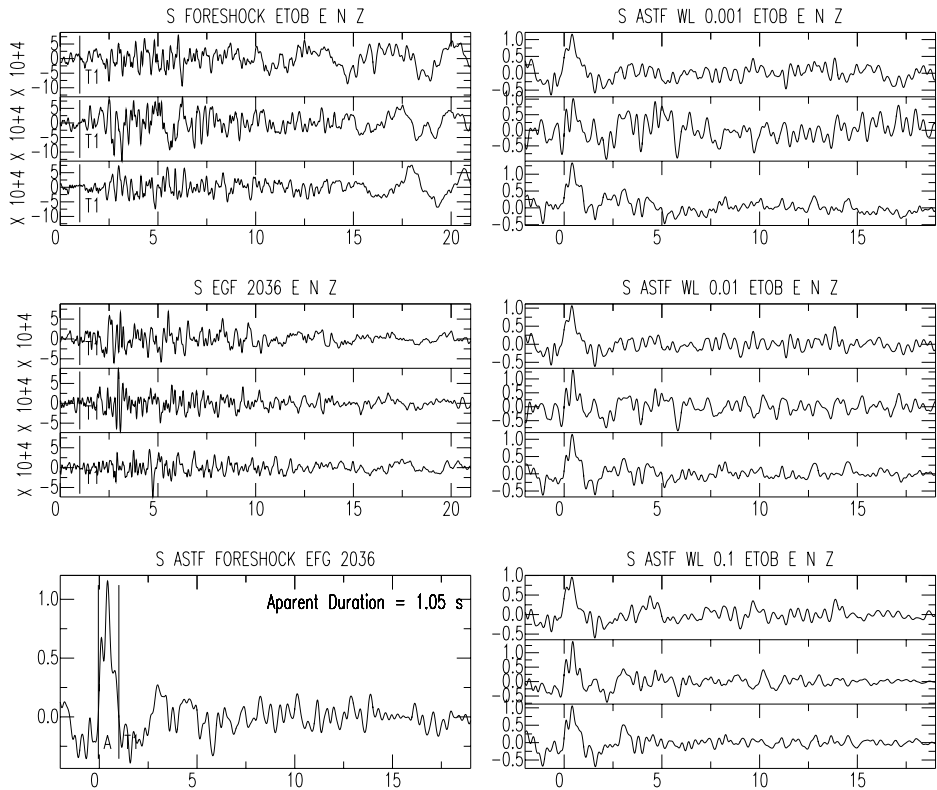
ETOB

Frequency domain deconvolution

P - wave



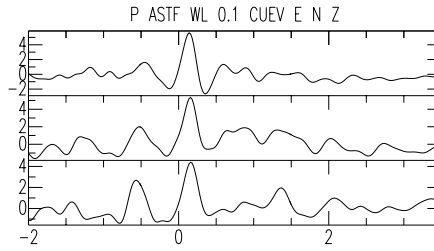
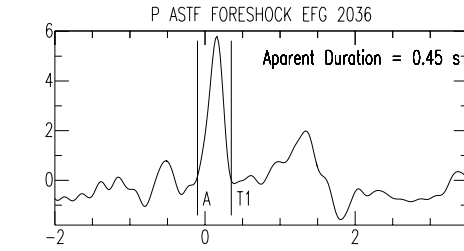
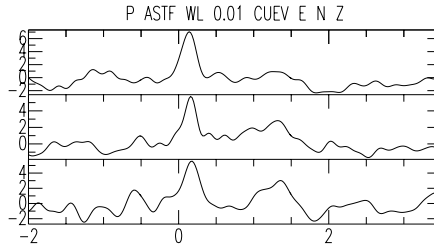
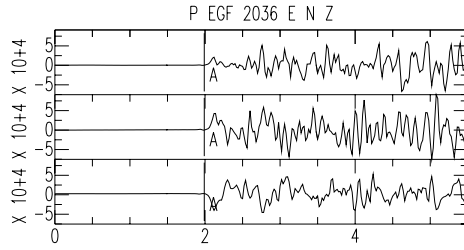
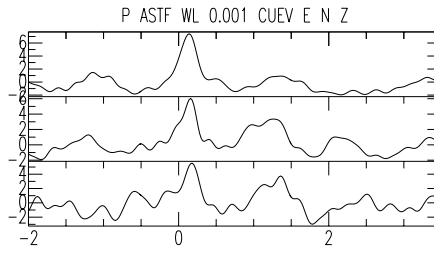
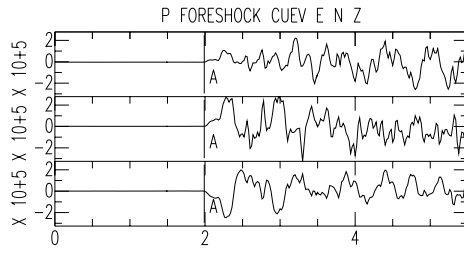
S - wave



CUEV

Frequency domain deconvolution

P - wave



S - wave

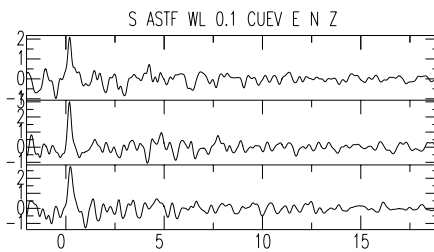
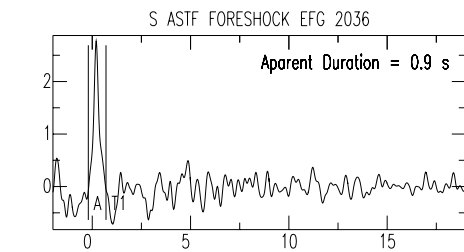
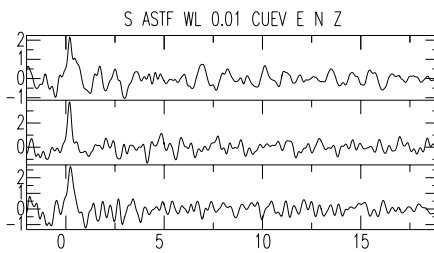
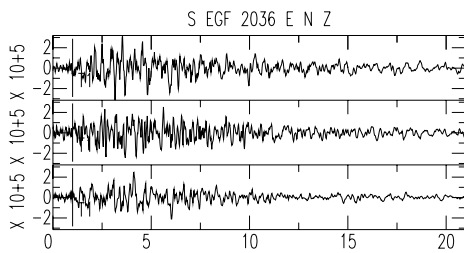
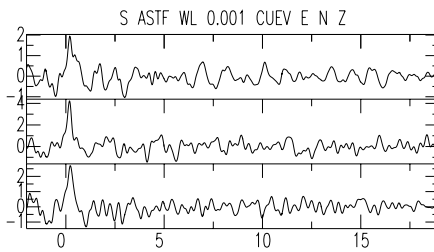
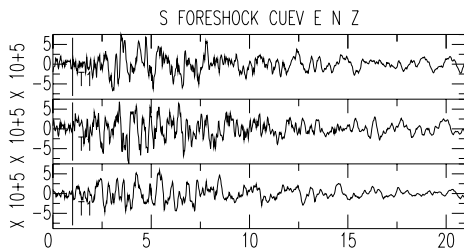


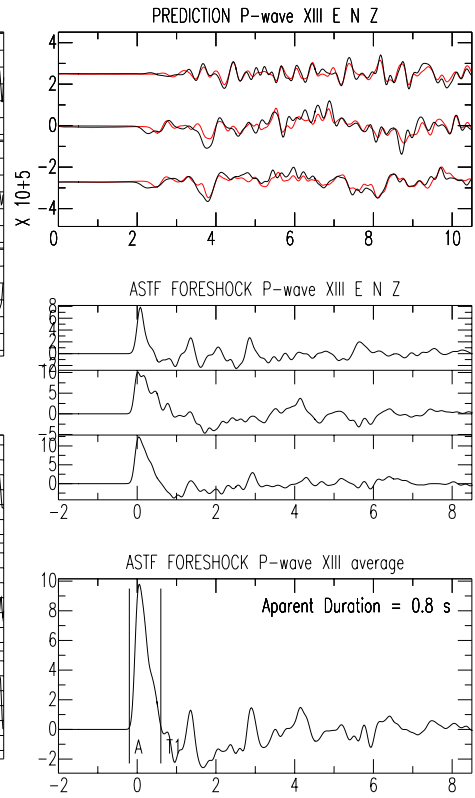
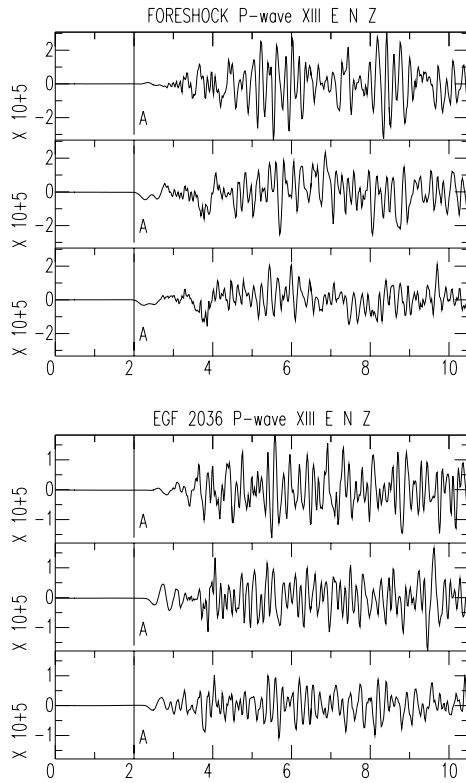
Figure S1: Frequency-domain deconvolution for the seismic station ETOB using P-waves (top panel) and S-waves (bottom panel) for the Mw 4.6 foreshock. The first column for each panel shows: original seismogram for the main event, i.e., the Mw 4.6 foreshock (top); Empirical Green Function (EGF), i.e., the greatest aftershock with Mw 3.9, denoted as “2036” in the title (middle); final Apparent Source Time Function (ASTF) from stacking of the results shown in the second column, indicating the duration’s measurements on the trace (bottom). The second column for each panel shows the calculated ASTFs with different water level values: 0.001 (top); 0.01 (middle); 0.1 (bottom). The boxes show the East- (E), North- (N) and vertical-component (Z) traces. Horizontal axis is in seconds.

Figure S1: continued: Frequency-domain deconvolution for the seismic station CUEV.

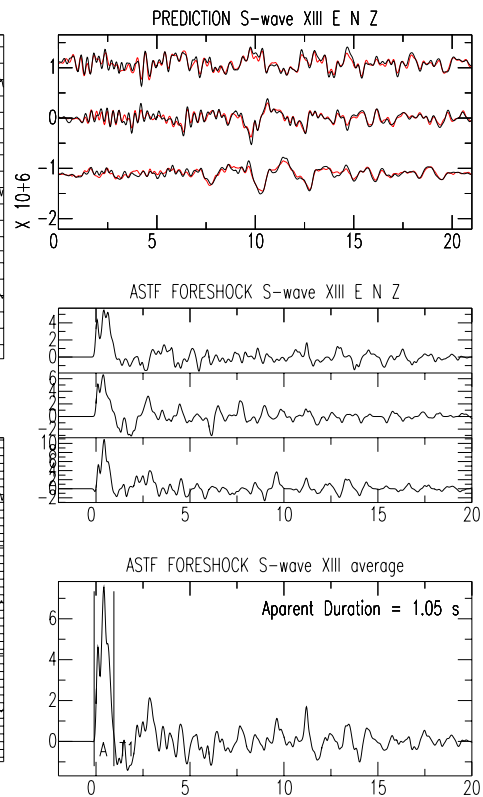
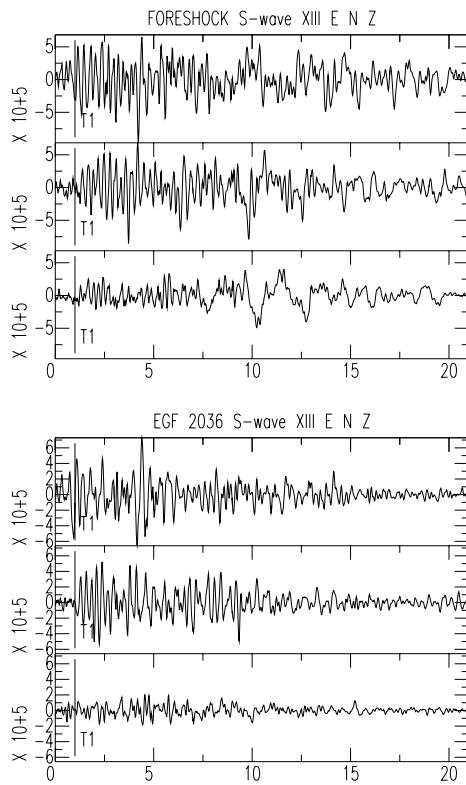
XIII

Time domain deconvolution

P - wave



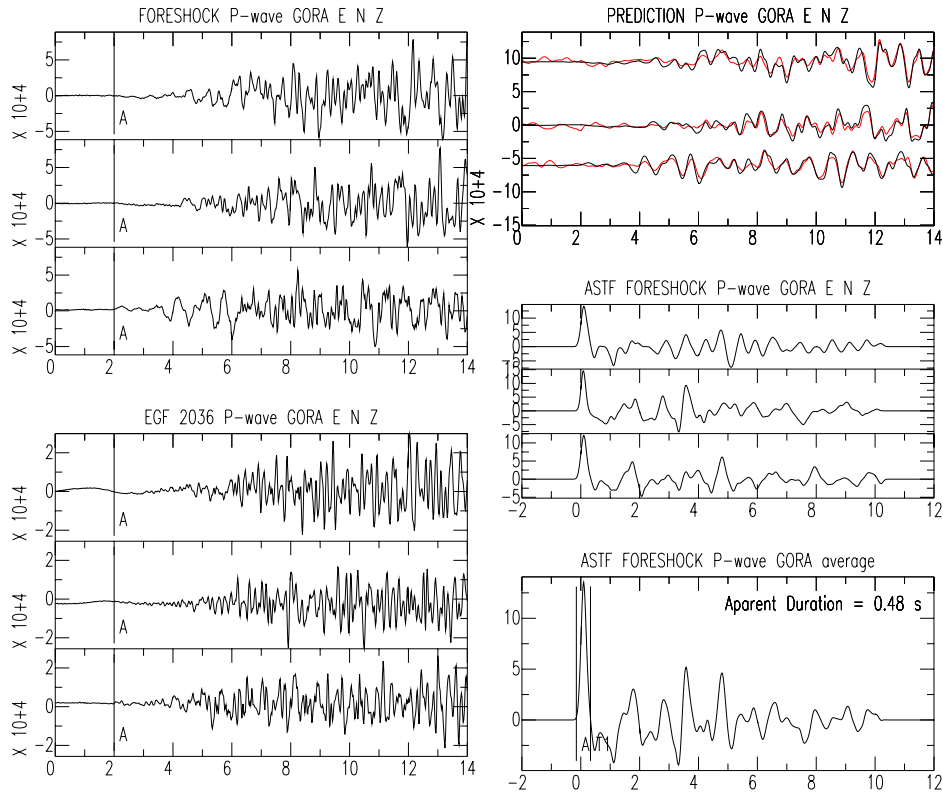
S - wave



GORA

Time domain deconvolution

P - wave



S - wave

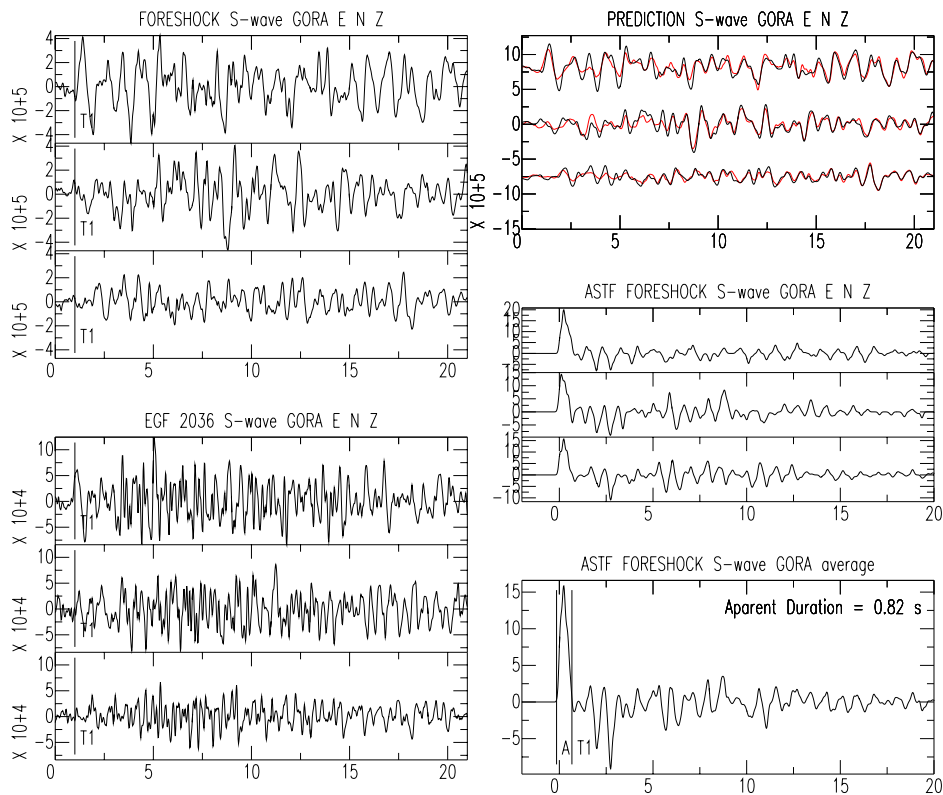


Figure S2: Time-domain deconvolution for the seismic station XIII using P-wave (top panel) and S-wave (bottom panel) for the Mw 4.6 foreshock. The first column for each panel shows: original seismogram for the main event, i.e., the Mw 4.6 foreshock (top); Empirical Green Function (EGF), i.e., the greatest aftershock with Mw 3.9, denoted as 2036 in the title (bottom). The second column for each panel shows: target seismogram (black trace, main event filtered using a Gaussian filter with a width factor of 10) and predicted seismogram (red trace) (top); ASTF for each component (middle); final ASTF from stacking, indicating the duration's measurements on the trace (bottom). The boxes show the East- (E), North- (N) and vertical-component (Z) traces. Horizontal axis is in seconds.

Figure S2: continued: Time-domain deconvolution for the seismic station GORA.

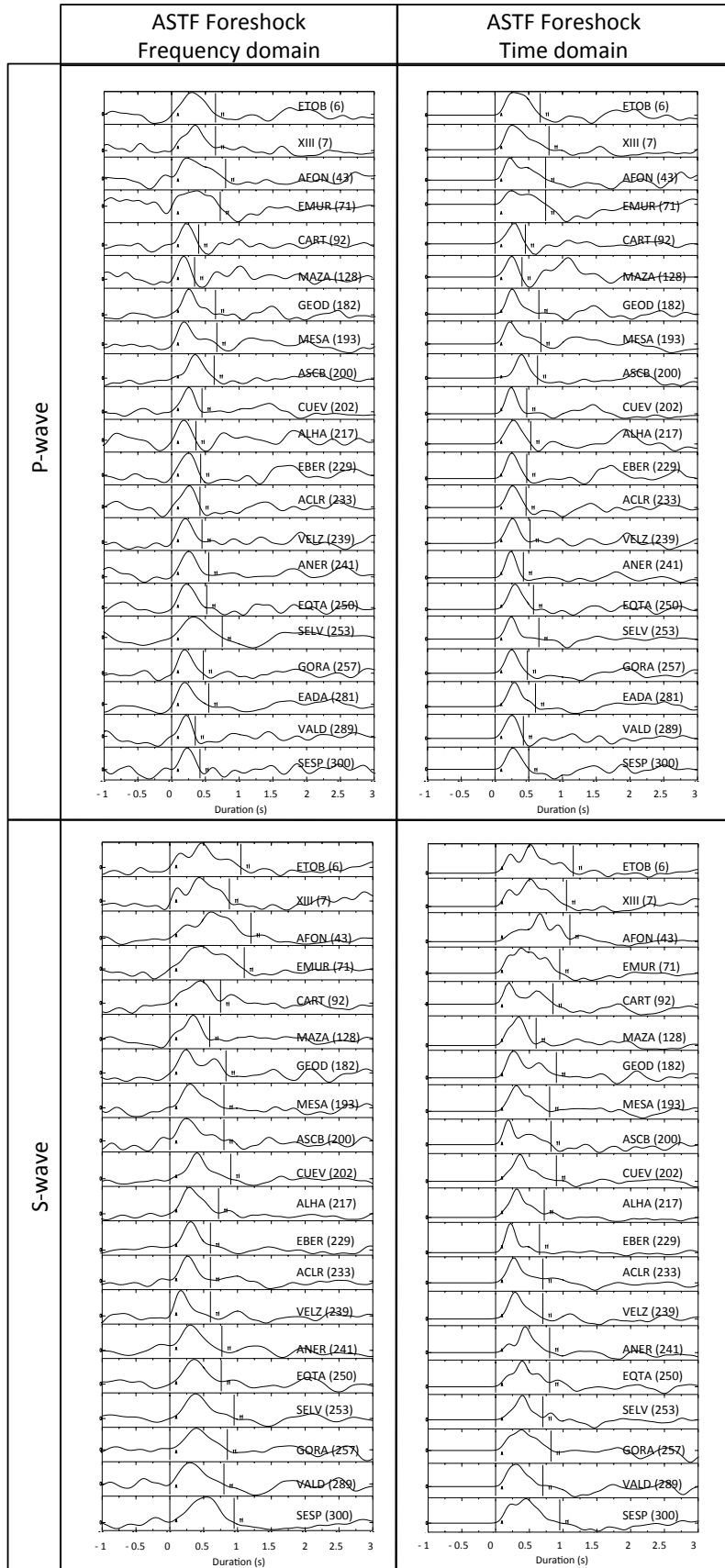


Figure S3. Apparent source time functions (ASTFs) for the Lorca Mw 4.6 foreshock. Deconvolved functions from P- and S-waves are shown, as well as the results from different deconvolution schemes (frequency deconvolution: left, time domain deconvolution: right). ASTFs are plotted in station's azimuthal order, showing a systematic variability of apparent source durations (the duration's measurements are indicated on the traces and in table S1). Labels indicate the station's name and the azimuth for each ASTF.

Seismic station	Azimuth (°)	ASTF durations (s)					
		P- wave			S-wave		
		Mainshock	Foreshock		Mainshock	Foreshock	
			Frequency	Time		Frequency	Time
ETOB	6.1	0.75	0.65	0.67	1.20	1.05	1.15
XIII	7.8	1.00	0.65	0.80	1.15	1.02	1.05
AFON	43.1	1.05	0.80	0.75	1.40	1.20	1.10
EMUR	71.7	1.00	0.72	0.75	1.30	1.10	0.95
CART	92.9	0.70	0.40	0.45	1.10	0.75	0.85
MAZA	128.7	0.65	0.34	0.40	0.80	0.59	0.60
GEOD	182.7	0.55	0.65	0.65	0.95	0.83	0.90
MESA	193.3	0.60	0.67	0.68	0.90	0.80	0.80
ASCB	200.8	0.55	0.63	0.63	1.00	0.80	0.82
CUEV	202.8	0.55	0.45	0.47	0.90	0.90	0.90
ALHA	217.4	0.45	0.36	0.53	0.80	0.72	0.72
EBER	229.7	0.60	0.43	0.47	0.90	0.60	0.65
ACLR	233.5	0.80	0.42	0.46	0.90	0.60	0.70
VELZ	239.6	0.80	0.45	0.52	0.95	0.60	0.70
ANER	241.5	0.60	0.55	0.42	0.80	0.77	0.80
EQTA	250.3	0.65	0.52	0.57	0.90	0.76	0.80
SELV	253.9	0.65	0.75	0.65	0.95	0.95	0.70
GORA	257.5	0.55	0.47	0.48	0.85	0.85	0.82
EADA	281.8	0.55	0.55	0.60	-	-	-
VALD	289.0	0.65	0.35	0.42	0.80	0.80	0.70
SESP	300.1	0.65	0.42	0.50	1.10	0.95	0.95

Table S1. ASTF durations and station's azimuth for the foreshock ($M_w = 4.6$) and mainshock ($M_w = 5.2$) Lorca earthquakes applying deconvolution to P-wave and S-wave windows. The results are calculated from different deconvolution schemes (frequency and time domain). Note that we obtain the same values of apparent durations for the mainshock with both deconvolution techniques.

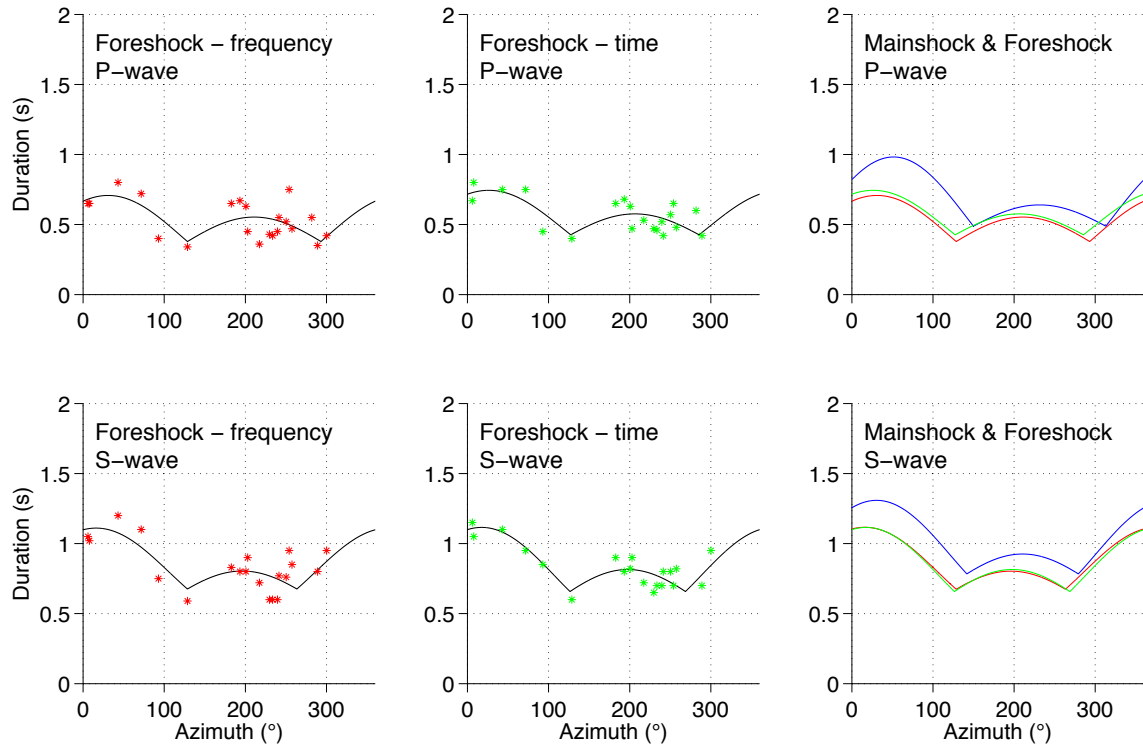


Figure S4. Inversion of apparent durations for the Lorca Mw 4.6 foreshock using a trust-region algorithm. The results are shown according to an asymmetric bilateral rupture for P-waves (first row) and S-waves (second row). The first and second columns show measurements (star symbols) and synthetic predictions (solid lines) for different deconvolution schemes: frequency domain (red) and time domain (green), respectively. The third column compares the predictions for Mw 4.6 (red and green solid lines take into account the previous deconvolution schemes) and 5.2 (blue solid line) Lorca earthquakes.

	Line source directivity analysis for the foreshock	
	Frequency domain	Time domain
Directivity (°)	204 ± 16	202 ± 11
Bilateral percentage (%)	60 ± 5	60 ± 3
Rupture velocity (km/s)	3.35 ± 3.90	3.15 ± 2.06
Rupture length (km)	2.26 ± 1.10	2.24 ± 0.98
Total rupture time (s)	0.87 ± 0.18	0.91 ± 0.16
Rise time (s)	0.2	0.2

Table S2. Inversion of apparent durations for the Lorca Mw 4.6 foreshock using a trust-region algorithm. The results are shown from different deconvolution schemes (frequency and time domain). The best-fitting value and their uncertainties are shown for each involved parameter.

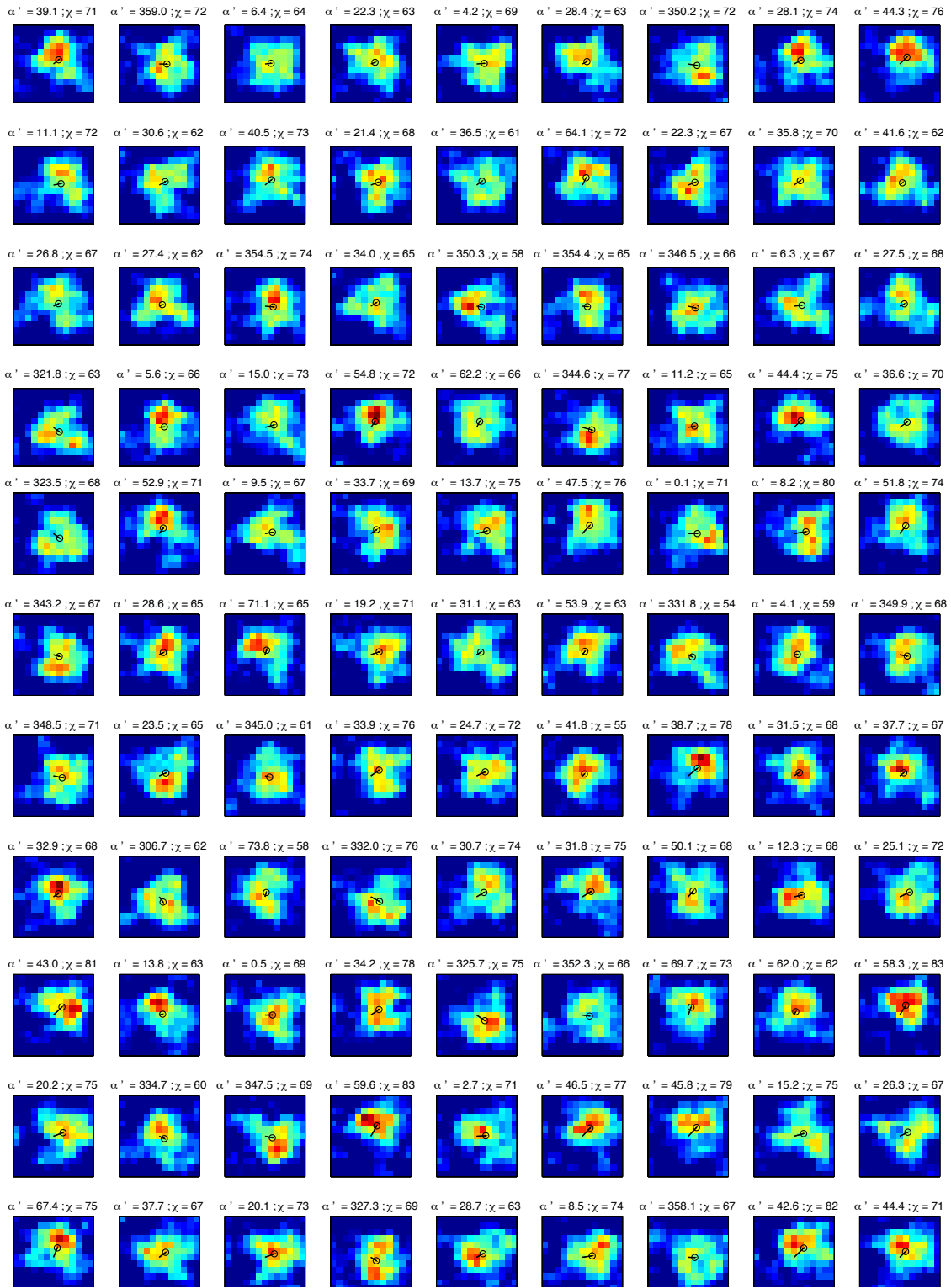


Figure S5. Solution ensemble from Popperian inversion for the 2011 Mw 4.6 Lorca (Spain) foreshock, consisting of 193 unfalsified trial models with L1-fit ≥ 0.6227 . Slip maps are sorted according to L1-fit in descending order. For each slip map we show the directivity vector from the hypocenter to the moment centroid (black open circle). Angle of the directivity vector in the rupture plane (α') in degrees and the asymmetry of rupture (χ) in percentage are labeled on top of the slip maps.

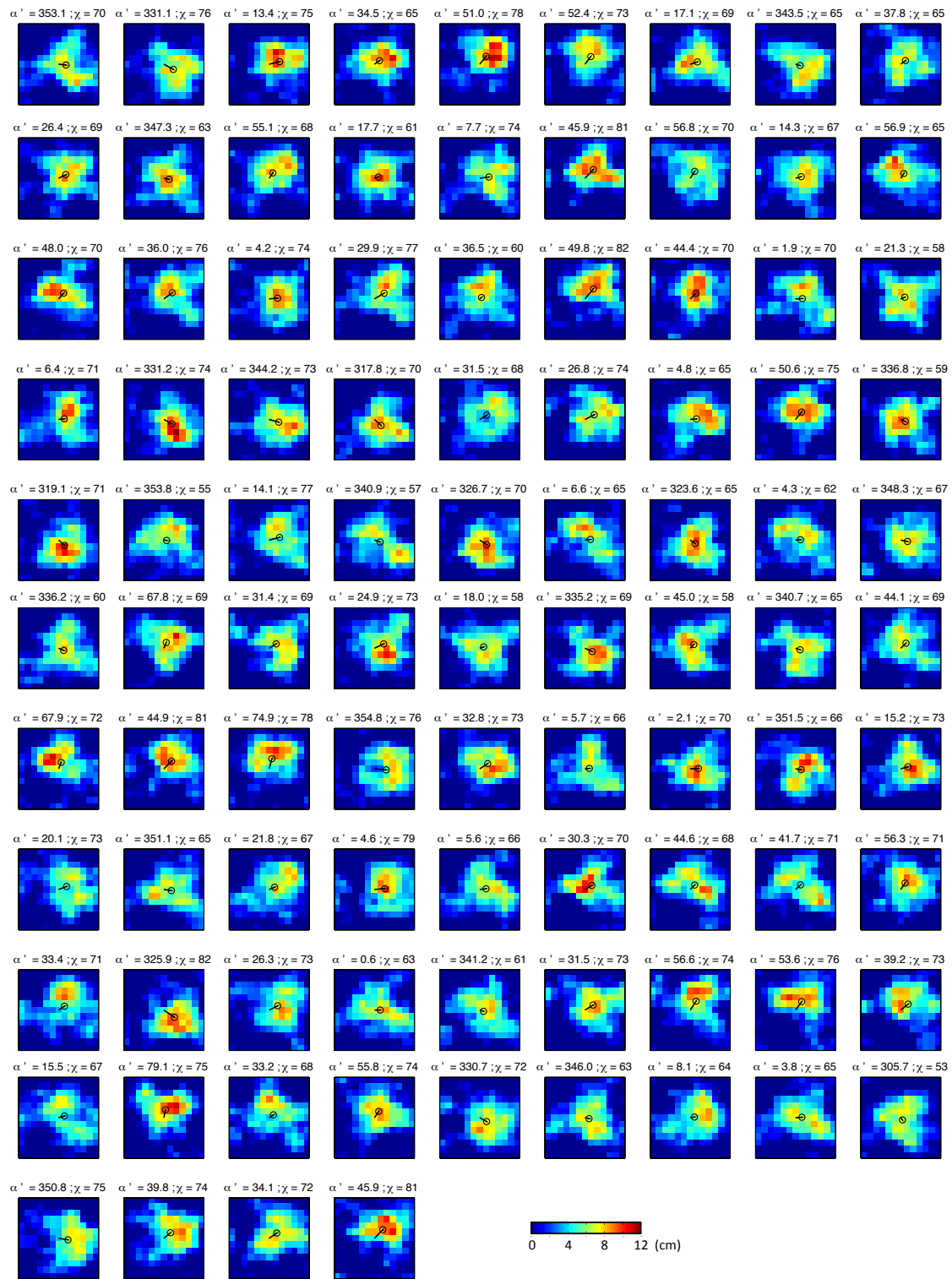


Figure S5. Continued.